# Super-Resolution Study of Polymer Mobility Fluctuations near *c**

John T. King,[†] Changqian Yu,[†] William L. Wilson,[†,‡] and Steve Granick[†,‡,§,⊥,∥,]*

[†]Department of Materials Science and Engineering, [‡]Materials Research Laboratory, [§]Department of Chemical and Biological Engineering, [⊥]Department of Chemistry, and [∥]Department of Physics, University of Illinois, Urbana, Illinois 61801, United States

ABSTRACT Nanoscale dynamic heterogeneities in synthetic polymer solutions are detected using super-resolution optical microscopy. To this end, we map concentration fluctuations in polystyrene—toluene solutions with spatial resolution below the diffraction limit, focusing on critical fluctuations near the polymer overlap concentration, *c**. Two-photon super-resolution microscopy was adapted to be applicable in an organic solvent, and a home-built STED-FCS system with stimulated emission depletion (STED) was used to perform fluorescence correlation spectroscopy (FCS). The polystyrene serving as the tracer probe (670 kg mol^{-1}, radius of gyration

$R_G \approx 35$ nm, end-labeled with a bodipy derivative chromophore) was dissolved in toluene at room temperature (good solvent) and mixed with matrix polystyrene (3,840 kg mol^{-1}, $R_G \approx 97$ nm, $M_w/M_n = 1.04$) whose concentration was varied from dilute to more than $10c*$. Whereas for dilute solutions the intensity—intensity correlation function follows a single diffusion process, it splits starting at *c** to imply an additional relaxation process provided that the experimental focal area does not greatly exceed the polymer blob size. We identify the slower mode as self-diffusion and the increasingly rapid mode as correlated segment fluctuations that reflect the cooperative diffusion coefficient, D_{coop}. These real-space measurements find quantitative agreement between correlation lengths inferred from dynamic measurements and those from determining the limit below which diffusion coefficients are independent of spot size. This study is considered to illustrate the potential of importing into polymer science the techniques of super-resolution imaging.
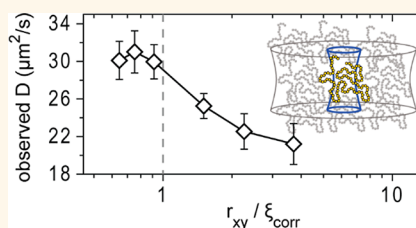
KEYWORDS: super-resolution spectroscopy · polymer dynamics · semidilute polymer solutions

The progression of polymer segment concentration (*c*), from dilute to semidilute to concentrated to melt, has interesting predicted consequences for concentration fluctuations.[1−3] We are interested here in the fact that as chains begin to reach overlap concentrations, critical fluctuations of segments emerge over extended distances. Scaling theory allows their length scale, the "blob" size, to be predicted given some empirical inputs (the radius of gyration, R_G, and the overlap concentration, *c**).[4] This scenario implies two orthogonal diffusive processes. Critical segmental fluctuations, driven by excluded volume repulsion, manifest themselves in the osmotic compressibility of the solution as chains are pushed together, and this produces the cooperative diffusion coefficient, D_{coop}, but the scale of cooperativity decreases as polymer concentration increases.[2] Near the overlap concentration, it is physically reasonable to expect the polymer solution to become a mosaic, some spatial regions enjoying free translational motion of chains that locally are in a dilute

regime, other spatial regions with strong concentration dependence as overlapping chains experience slower, more restricted mobility. As the polymer concentration increases chain entanglements begin to constrain the cooperative fluctuations, limiting correlated motion to increasingly smaller pockets according to the scaling laws that describe cooperative diffusion.[2]

More than 30 years ago, experimental measures of segmental dynamics within correlated regions, expressed as the cooperative diffusion coefficient D_{coop}, were obtained using dynamic light scattering.[5] Relating this to the correlation length ξ through the Stokes—Einstein relation $D_{coop} = k_B T/6\pi\eta_s\xi_{coor}$, the observation $D_{coop} \sim c^{0.75}$ was found to agree with the prediction from scaling theory, $\xi_{corr} \sim R_G(c/c*)^{-0.75}$.[1,2,5] Physically, one expects maximum effect when $\xi_{corr} \sim R_G$ at the overlap concentration, as higher concentrations are accompanied by local entanglement that progressively limit correlated fluctuations to smaller and smaller length scales. However, because of the intrinsic scale of segmental motion in
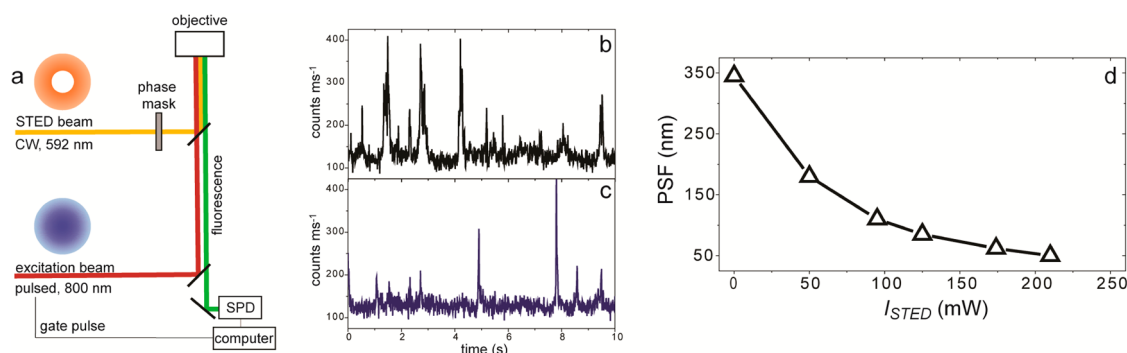
Figure 1. Experimental setup. (a) Schematic depiction of the home-built time-gated STED-FCS used in this study. Two-photon absorption in the sample is excited by a pulsed 800 nm laser. To produce subdiffraction spot size, the depletion beam from a 592 nm CW laser passes through a phase plate that gives it a doughnut shape, leaving only dye molecules in the zero-intensity center capable of visible fluorescence. Fluorescence fluctuations for dye labeled nanoparticles with diffraction limited spot **(b)** and a STED generated spot of roughly 60 nm **(c)**. The duration of the fluorescent bursts decrease significantly as the spot size is reduced, though the intensity of the fluorescent bursts remains roughly the same. For the bodipy dye used in these experiments, the point-spread function is plotted against I_{STED} **(d)**. Notice that the smallest focal PSF, equivalent to the smallest focal diameter, is ∼60 nm.

synthetic polymers being below the diffraction limit, there has been no real-space confirmation of this.

The rapidly advancing field of super-resolution imaging[6,7] offers an experimental approach to test these and related matters in the field of polymer science. Here, we use STED (stimulated emission depletion), as it is considered to lend itself especially well to studying time-dependent changes. To date, dynamic studies using STED focused on biological systems.[8,9] We explore its utility to address problems in materials science, specifically (in this study) to study the segmental motion of polymer chains whose size falls below the conventional diffraction limit.[10−13] We couple it to fluorescence correlation spectroscopy (FCS) of mono end-labeled fluorescent polymer chains. The focused two-photon beam creates an illuminated spot with a beam waist that we vary from at most 300 μm while the small number of fluorophores contained within a given volume (at most 3−10) fluctuates as polymers diffuse in and out. The fit to the autocorrelation function determines the diffusion of the fluorescing species such that the diffusing dye reports on diffusion of the polymer chains. The combination, STED-FCS, is particularly attractive because spatial resolutions upward of 10 times less than the diffraction limit can be obtained without sacrificing the temporal resolution that is standard for FCS, making it attractive for dynamic studies on the nanoscale.

RESULTS AND DISCUSSION

Figure 1a shows a schematic diagram of the STED-FCS experimental setup. A confocal geometry is used to excite a diffraction limited spot of fluorophores. To implement the STED phenomenon, a second beam, tuned to the emission wavelength, is aligned to be collinear with the excitation beam. By passing the depletion beam through a vortex phase mask the beam acquires a "doughnut" shape, with a high intensity ring

of light and a zero intensity center. The depletion beam stimulates emission from molecules within the high intensity ring and, due to the phase matching condition, causes the stimulated emission to be emitted in the same direction as the depletion beam, leaving it undetected. Dyes in the zero-intensity region of the depletion beam are left to spontaneously fluoresce, and the size of this region is not spatially limited by diffraction.

While one might be tempted to worry that the relatively small excitation volume reduces signal-to-noise of the signal, this is not so because FCS measures fluctuations rather than background. An example is shown in Figure 1b,c, representative graphs of fluctuation counts plotted against time. Comparing these for a diffraction-limited FCS spot, and a smaller spot of size 60 nm, this raw data shows no cost in signal-to-noise, though fluctuations are naturally fewer in the latter case. Furthermore, because the depletion efficiency is proportional to the STED beam power, the spot size (d_{xy}) can be systematically varied.[6] For example, a plot of the point spread function (nm) against intensity of the STED excitation (Figure 1d) shows how the former can be varied from the diffraction limit of ∼345 nm down to progressively lower values. The smallest size in the present study was 60 nm, though spot sizes as low as 20 nm using molecular dyes have been reported.[14] Coupling this excitation scheme with the established technique of FCS allows diffusive dynamics on the nanoscale to be accessed.[15] The Experimental Section describes techniques that were developed, in the course of this study, to apply STED-FCS to study polymers in organic solution.

This experiment was designed such that the radius of gyration of the host polymer exceeded the STED d_{xy}, and thus, internal motion would be observed. Figure 2a shows a cartoon describing a semidilute polymer solution at the overlap concentration; while translational
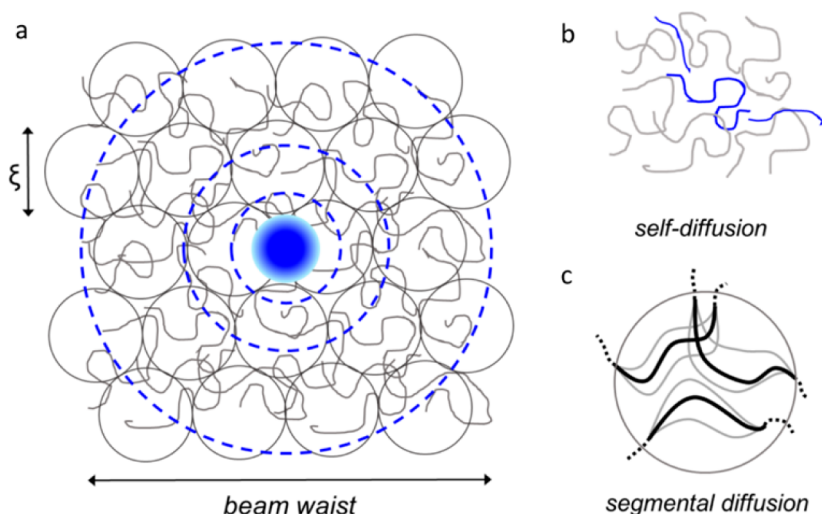
Figure 2. (a) Cartoon showing a semidilute polymer solution at the overlap concentration with close-packed circles representing what polymer physics jargon refers to as the "blobs" of polymer segments. The spot sizes, or beam waists, used in the experiments are shown in blue, with the scaling between the correlation length and the spot size being roughly correct. Within the blobs, the segmental dynamics (c) are correlated and described by a cooperative diffusion coefficient, D_{coop}. It is distinct from the translational motion of the polymer chains through the environment (b), quantified by the self-diffusion coefficient, D_{self}.

motion of the polymer chains is described by a different diffusion coefficient, that of the chain's center of mass (Figure 2b), it is different at smaller scale. Within what the field of polymer physics refers to as "blobs", the segmental dynamics (Figure 2c) are described by a cooperative diffusion coefficient. To analyze the FCS data, first the intensity–intensity autocorrelation function was calculated and the $G(\tau = 0)$ value was normalized to unity, as is standard for this technique, giving the autocorrelation function, $G(\tau)$, as a function of logarithmic time lag, τ. Note that as the principle of an FCS measurement is to analyze rate of fluctuation, signal-to-noise in this experiment improves with decreasing spot size. Moreover, the orthogonality of diffusion in the three Cartesian directions (x, y, and z) explains why 3D diffusivity is inferred from measurements projected into the 2D xy plane.

FCS Experiments with Diffraction-Limited Spot Size. The raw data with conventional FCS ($d_{xy} = 345$ nm) are summarized in Figure 3a. At every polymer concentration, the autocorrelation curves were fit to the known form for a single diffusion process, and also to the known form for a two-component diffusion process (see Supporting Information). The way to read these curves is that they show the delay time required for the polymer-attached dyes to diffuse a distance roughly equal to d_{xy}. While strict calculation also takes into account the Gaussian intensity profile of the excitation beam, the translational diffusion coefficient is approximately the square of d_{xy} divided by the characteristic time.[16]

Provided that only the extremes of dilute and concentrated concentrations are considered, the data are simple to interpret. Regardless of whether one allows one relaxation process or two, the fits are nearly identical, the negligible residuals from the alternative fits reflecting only noise in the data (Supporting Information). But starting at relative concentration $c/c^* = 1.25$, $G(\tau)$ is significantly better described by two components. The unacceptable fit from the alternative hypothesis of a one-component process is clear from the residuals (Supporting Information), which shows structure beyond signal noise for concentrations near c^*. At this stage of the experiments, we tentatively assigned the faster relaxation time to correlated segmental fluctuations, the slower relaxation time to self-diffusion.[5] The fluctuations are not spatially resolved, but nonetheless, the Gaussian intensity profile of illumination and bleaching can produce edge effects, specifically situations in which dyes located near the edge of the focal spot can register fluorescent bursts without traversing the focal volume. In the biophysics community, there is a tradition of fitting segmental motion of polymers measured by FCS to models based on assuming a diffusive process and we followed this approach.[17]

The implied diffusion coefficients of the fast mode, D_{coop}, and the slow mode, D_{self}, are summarized in Figure 3b, plotted for 345 and 60 nm spot sizes as a function of concentration on log–log scales. In the inset, their ratio is plotted against logarithmic concentration. The scaling of D_{self} is consistent with other FCS studies of self-diffusion in polystyrene systems.[18−20] In dilute and concentrated solutions, the cooperative diffusion cannot be resolved but the ratio rises abruptly at c^* (that the effect is observed so close to the definition of c^* is remarkable, as the definition of c^* naively supposes polymer coils at c^* to be close-packed spheres). As the concentration is further increased, D_{coop} is predicted to grow as $c^{0.75}$ but on increasingly
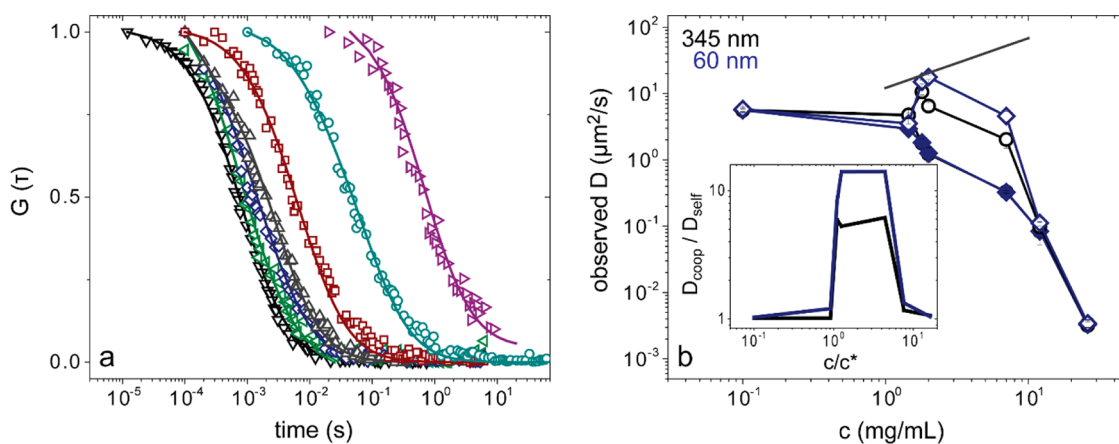
Figure 3. Examples of raw data. (a) Traditional FCS. Using traditional diffraction-limited spot size, the normalized intensity−intensity autocorrelation function is plotted against logarithmic time lag for end-labeled PS in toluene under the conditions described in the text. Data was collected for $c/c* \sim$ 16.25 (purple), 7.62 (cyan), 4.40 (red), 1.25 (gray), 1.10 (navy), 0.91 (green), as well as in dilute solution (black). Polymer concentrations are identified in the inset. The solid lines are 2-component fits to the data as described in the Supporting Information. This provides the most consistent fits throughout the concentration series, giving two diffusion coefficients at each concentration, D_{self} and D_{coop}, except that D_{coop} seems to be only resolved at $c > c*$, where the correlation lengths are large. (b) STED-FCS. Diffusion coefficients for two spot sizes, 345 and 60 nm, are plotted against polymer concentration on log−log scales. The dashed line shows the expected scaling for D_{coop} with concentration. As the concentration is increased the length scale of cooperative diffusion decreases, and the spatial resolution provided by STED-FCS is no longer sufficient to measure accurate diffusion coefficients. The inset shows the ratio D_{coop}/D_{self} as a function of concentration.
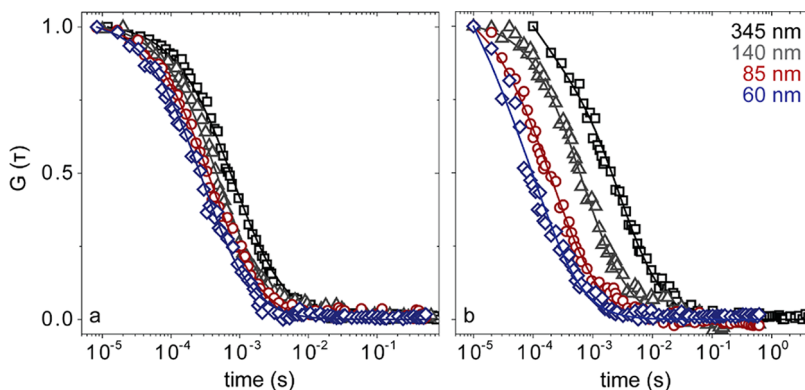

Figure 4. STED-FCS autocorrelation functions for dilute polymer solutions (a) and the semidilute solutions at $c/c* = 1.25$ (b). As d_{xy} of the excitation laser is downsized the curves shift to shorter time scales because it takes less time for molecules to diffuse through the spot.

smaller length scales and with increasingly rapid decrease of intensity−intensity autocorrelations.[5] The apparent decrease of D_{coop} at high concentration measured here is not real; it reflects simply that the length scale of the correlated fluctuations is far below our spatial resolution and we cannot distinctly resolve these motions (see the Supporting Information).

STED-FCS Experiments. STED experiments were performed with beam diameters of 140, 85, and 60 nm. Illustrative raw data are shown in Figure 4a,b, autocorrelation functions plotted against logarithmic time lag with varying d_{xy} for dilute solution and $c/c* \approx 1.25$, respectively. As d_{xy} is reduced, the autocorrelation function decays more quickly, as less time is needed for probe molecules to diffuse through the focal volume.[15] For a freely diffusing molecule, the diffusion constant is independent of d_{xy}, as its diffusion looks

similar on any length scale. For a molecule diffusing through a system with nanoscale heterogeneity, the observed diffusion constant can have a nontrivial dependence on the length scale probed.[8,21,22]

The dependence on d_{xy} of the apparent diffusion coefficient is plotted in Figure 5 for all the polymer concentrations that we studied. Translational diffusion, D_{self}, shows no dependence (Figure 5a). It is at first surprising that this trend persists up to the highest concentrations, a condition when one would expect the dominant mode of translational diffusion to be reptation, which would not be Fickian over our time scale (tens of seconds). It is possible that the dominant mode of motion does indeed occur through a process more complicated than free diffusion but that the length scales for heterogeneity would be too small to observe with STED-FCS.
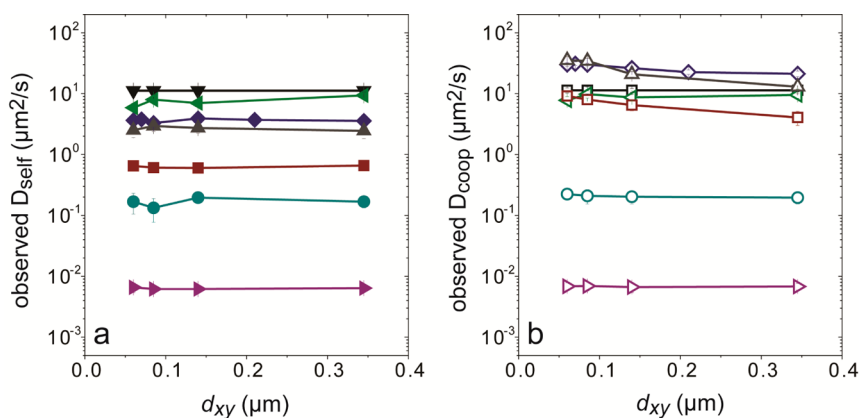
Figure 5. Quantification of dependence on spot size. (a) Slow component of autocorrelation function decay, which we identify with D_{self}, plotted semilogarithmically against focal diameter. The lack of dependence suggests free diffusion on the length scales studied here. Similar data at other concentrations, below and well above c^*, likewise show no dependence. (b) Faster component of autocorrelation function decay, which we identify with D_{coop}, plotted semilogarithmically against focal diameter. The main observation presented here is the independence of D_{self} on d_{xy} as well as the independence of D_{coop} on d_{xy} in the dilute and concentrated regimes. Polymer concentrations around c^* show a strong increase in this diffusion coefficient as the focal diameter decreases, which is highlighted in Figure 6. Data were collected for $c/c^* \sim 16.25$ (purple), 7.62 (cyan), 4.40 (red), 1.25 (gray), 1.10 (navy), 0.91 (green), as well as in dilute solution (black).
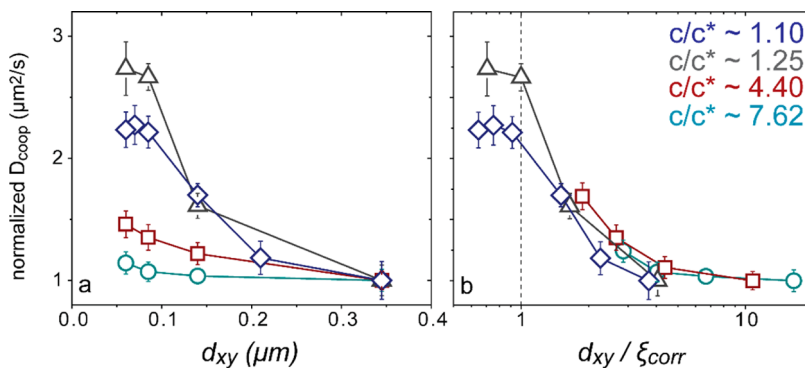

Figure 6. Magnified consideration of how D_{coop} depends on d_{xy} at polymer concentrations near c^*, after normalizing the data to be the same at the largest d_{xy}. (a) Plots as a function of d_{xy}. Below a critical focal diameter the data is independent of focal diameter but decreases when the focal diameter is larger. The dashed vertical lines compare to the correlation lengths predicted at each concentration from scaling theory. The expected plateau is observed for the two smallest concentrations. (b) The same data plotted as a function of d_{xy} normalized by the correlation length, ξ_{corr}.

In contrast, D_{coop} depends on d_{xy} for solutions near c^*, increasing steadily as d_{xy} decreases (Figure 5b). This arises because local segmental dynamics are significantly faster than self-diffusion. So long as the beam size is the blob size or smaller, segmental dynamics are discriminated and an accurate value of D_{coop} is obtained. When the beam size is larger than the blob size a diffusion coefficient that is erroneously small is measured.

To highlight the dependence on d_{xy}, the data at every concentration were shifted on the vertical scale to agree at largest d_{xy}. With this normalization, the behavior of D_{coop} near c^* is summarized in Figure 6. The normalized data are plotted against linear focal diameter (panel a) and against focal diameter normalized to the correlation length (panel b). With decreasing focal diameter, the inferred diffusion coefficient increases up to a plateau beyond which it is constant. The turnover point provides direct spatial mapping of the size of cooperative regions. However, standard

scaling theory also predicts the correlation lengths that describe the predicted blob sizes, and these are included as vertical dashed lines in Figure 6 (see the Supporting Information). At $c/c^* \approx 1.10$, the predicted correlation length is ~93 nm, and the observed D_{coop} indeed shows a turnover at this focal diameter. Likewise, at $c/c^* \approx 1.25$, the turnover point is at smaller focal diameter, roughly 80 nm, and this is accompanied by a higher level of D_{coop} in the plateau region. This agrees with theory, which predicts that increasing concentration causes cooperative fluctuations to speed up though they are confined to smaller length scales.[1,4,5] For these two concentrations we are able to spatially resolve the cooperative regions, but for the other solutions studied here the correlation length is too small to be resolved.

The trends shown in Figure 6a,b can be rationalized by a consideration of semidilute polymer systems. The principle idea of these experiments is that cooperative fluctuations can be accurately measured if d_{xy} is

reduced to the domain size, or correlation length. As d_{xy} approaches the correlation length (ξ_{corr}), the co-operative fluctuations, which have a higher diffusion coefficient than the translation motion, are more fully resolved, and thus the observed diffusion coefficient increases. When $d_{xy} \sim \xi_{corr}$ the cooperative diffusion can be fully resolved and the observed D_{coop} will not be convoluted with the slower D_{self}, leading to an accurate measure of D_{coop} at the plateau region of the data.

The constraint of experimental resolution is why matrix polymers of such high molecular weight were used—we sought to maximize the correlation length of the polymer solutions. Control experiments were performed in which the same probe polymer was embedded in a matrix of matched molecular weight, PS 706 kg mol^{-1}. The experimental findings were consistent qualitatively: emergence of two-component relaxation near c^* and increase in D_{coop} with decreasing d_{xy}, but for this polymer the maximum expected correlation length is on the order of 40 nm, below the optical resolution obtainable with our setup. The two sets of results, taken together, suggest the interpretation that in determining the scaling of cooperative diffusion of probe chains, the relevant correlation length was close to that of the matrix chains.

In the same spirit as standard in dynamic light scattering, these data also allow one to estimate the correlation length through a Stokes−Einstein relation.[5] For those instances where we access the plateau limit, the observed D_{coop} should be the true cooperative diffusion coefficient, which can then be used to estimate the correlation length through the Stokes−Einstein

relation. By this argument, the diffusion constants at $c/c^* \approx 1.10$ and $c/c^* \approx 1.25$ give correlation lengths $\xi \approx 91$ and 77 nm, which agree extremely well with the spatial measures of ~90 and 80 nm, respectively. In reaching this conclusion, we relied on measurements such that for each spot diameter the data were typically collected at 10 locations in the sample cell, each data set for 30−50 s, then averaged for analysis.

More generally, this comparison demonstrates the use of super-resolution FCS to study segmental dynamics on the nanoscale with quantitative precision.

CONCLUSION

Anticipating that super-resolution microscopy can become a useful experimental tool in materials science[23,24] just as it is already in the field of biophysics, this laboratory has undertaken consideration of scientific problems in which super-resolution microscopy can be applied usefully. In contrast to the biophysical emphasis on taking nanoscale images,[25−27] here we applied the approach to study nanoscale fluctuations occurring on length scales below the diffraction limit. It is also clear that the d_{xy} dependence we report here could lead to inaccurate measures of diffusion coefficients, highlighting the significance of continuing to explore super-resolution techniques to study nanoscale dynamics.

Looking beyond the specific experimental system studied here, this study is considered to demonstrate that STED-FCS provides a general avenue to spatially resolve heterogeneous dynamics in complex, nonbiological systems.

EXPERIMENTAL SECTION

STED-FCS Setup. We constructed a home-built time-gated STED with two-photon excitation, depicted schematically in Figure 1. Fluorescent dyes are excited using 800 nm pulses from a femtosecond laser (Spectra Physics Mai Tai). A depletion beam (592 nm CW laser, MPB Communications) tuned to the emission wavelength of the fluorophores is overlapped with the excitation profile, which is first passed through a vortex phase mask which gives the beam a doughnut shape.

FCS measurements made here rely on a stationary excitation spot focused into a dilute sample of fluorescent dyes.[13] As dyes diffuse through the excitation beam they fluoresce, which is detected on a single-photon counter (ID Quantique). Taking a correlation function of the intensity fluctuations gives the relaxation decay that can be related to a diffusive coefficient.[13,28] With STED-FCS, diffusive motion can be studied on various length scales. It extends to length scales well below the diffraction limit.

Applying STED-FCS To Study Polymers in Organic Solution. The covalent attachment of dye to polystyrene enables us to use fluorescent dye as a passive reporter of the segmental dynamics of those flexible polymer chains. However, selection of dye was at first problematical as most of the prior work utilizing STED was on biological systems. There exists a nice collection of literature on what dyes work well in aqueous environments, and what resolutions can be obtained using them,[14,29−32] but concerning the selection of dyes soluble in organic solvent, less was known. A limiting factor in the wide-implementation of

STED nanoscopy is the discovery of suitable dyes, which is often based on trial and error. The reason follows from considering the complexity of photophysics in this experiment. In addition to the requirement that the wavelengths of excitation and emission match the excitation and depletion beams that are available experimentally, alternative excited states can compete with the depletion process and render dyes unsuitable for STED experiments. These properties are almost impossible to predict based merely on inspection of molecular structure, so the most efficient way to find dyes suitable for experiments is trial and error.

Screening led us to discover that boron−dipyrromethene (BODIPY) dyes provide an excellent class of dyes for studying nonpolar solvents using STED under our experimental conditions. The point spread function of the BODIPY dye we used is shown, as a function of STED beam intensity, in Figure 1b. To calibrate the d_{xy}, we used STED-FCS data for our end-labeled polystyrene sample in dilute solution, assuming that its translational diffusion coefficient determined in dilute solution from FCS was independent of d_{xy}. The maximum resolution obtained was roughly 60 nm in the x−y plane, close to six times less than the diffraction limit, and roughly 360 nm in the z direction.[33]

Fluorescent traces were collected using time windows of roughly four decades of time, with maximum time delay on the order of 50 s. The needed data acquisition time for STED-FCS was the same as for conventional diffraction-limited FCS.

Polystyrene Samples in Toluene. We selected the model system, linear polystyrene in toluene, a good solvent. We began by

obtaining end-functionalized polymer with molecular weight as high as we could find. Carboxy-terminated polystyrene (M_w = 670 kg mol^{-1}, M_w/M_n = 1.06, Polymer Source) was coupled with a hydrazide-functionalized BODIPY derivative chromophore (BODIPY FL Hydrazide, Life Technologies). The reaction was carried out in THF with a coupling agent N,N'-dicyclohexylcarbodiimide, and the final product was purified by repeated precipitation with methanol. The labeled chains were normally dispersed (labeled chain concentration on the order of 10 nM) in an unlabeled sample of polystyrene (M_w = 3840 kg mol^{-1}, M_w/M_n = 1.04, Tosoh Corp.) in toluene (Sigma-Aldrich, >99.9%). When the aim was to study "dilute" solution, we studied only a small amount of the labeled polymer and the unlabeled PS was not added, giving a total concentration of ~10 nM. In control experiments (Supporting Information), we also used a matrix of unlabeled polystyrene with closely matched molecular weight (M_w = 706 kg mol^{-1}, M_w/M_n = 1.05, Tosoh Corp.).

Quantification of Polymer Overlap. Experiments were made over the concentration range from isolated chains to entangled (16 c^*), having estimated $c^* = 3M_n/4\pi N_A R_g^3$, where R_G of the unlabeled polymer which serves as the matrix is estimated from the empirical formula for polystyrene in toluene, $R_G \approx 0.012 M_w^{0.595}$, as 97 nm.[34]

Conflict of Interest: The authors declare no competing financial interest.

Supporting Information Available: Experimental fits of single-component and two-component relaxation of the FCS curves, comparison of the experimental data with expected scaling laws, and experiments performed using PS 700 K as the host polymer. This material is available free of charge *via* the Internet at http://pubs.acs.org.

REFERENCES AND NOTES

1. de Gennes, P. G. *Scaling Concepts in Polymer Physics*; Cornell University Press: Ithaca, 1979.
2. Doi, M.; Edwards, S. F. *The Theory of Polymer Dynamics*; Clarendon Press: Oxford, 1986.
3. Brown, W.; Nicolai, T. Static and Dynamic Behavior of Semidilute Polymer-Solutions. *Colloid Polym. Sci.* **1990**, *268*, 977–990.
4. de Gennes, P. G. Dynamics of Entangled Polymer-Solutions. 1. Rouse Model. *Macromolecules* **1976**, *9*, 587–593.
5. Adam, M.; Delsanti, M. Dynamical Properties of Polymer-Solutions in Good Solvent by Rayleigh-Scattering Experiments. *Macromolecules* **1977**, *10*, 1229–1237.
6. Hell, S. W. Far-Field Optical Nanoscopy. *Science* **2007**, *316*, 1153–1158.
7. Schermelleh, L.; Heintzmann, R.; Leonhardt, H. A Guide to Super-Resolution Fluorescence Microscopy. *J. Cell Biol.* **2010**, *190*, 165–175.
8. Eggeling, C.; Ringemann, C.; Medda, R.; Schwarzmann, G.; Sandhoff, K.; Polyakova, S.; Belov, V. N.; Hein, B.; von Middendorff, C.; Schoenle, A.; Hell, S. W. Direct Observation of the Nanoscale Dynamics of Membrane Lipids in a Living Cell. *Nature* **2009**, *457*, 1159–1162.
9. Andrade, D. M.; Clausen, M.; Lagerholm, B. C.; Hell, S. W.; Eggeling, C. Lipid Hop Diffusion on the Plasma Membrane - a STED-FCS Investigation. *Biophys. J.* **2013**, *104*, 193A–194A.
10. Shusterman, R.; Alon, S.; Gavrinyov, T.; Krichevsky, O. Monomer Dynamics in Double- and Single-Stranded DNA Polymers. *Phys. Rev. Lett.* **2004**, *92*, 048303.
11. Petrov, E. P.; Ohrt, T.; Winkler, R. G.; Schwille, P. Diffusion and Segmental Dynamics of Double-Stranded DNA. *Phys. Rev. Lett.* **2006**, *97*, 258101.
12. Enderlein, J. Polymer Dynamics, Fluorescence Correlation Spectroscopy, and the Limits of Optical Resolution. *Phys. Rev. Lett.* **2012**, *108*, 108101.
13. Woell, D. Fluorescence Correlation Spectroscopy in Polymer Science. *R. Soc. Chem. Adv.* **2014**, *4*, 2447–2465.
14. Westphal, V.; Hell, S. W. Nanoscale Resolution in the Focal Plane of an Optical Microscope. *Phys. Rev. Lett.* **2005**, *94*, 143903.
15. Kastrup, L.; Blom, H.; Eggeling, C.; Hell, S. W. Fluorescence Fluctuation Spectroscopy in Subdiffraction Focal Volumes. *Phys. Rev. Lett.* **2005**, *94*, 178104.
16. Rigler, R.; Mets, U.; Widengren, J.; Kask, P. Fluorescence Correlation Spectroscopy with High Count Rate and Low-Background-Analysis of Translational Diffusion. *Eur. Biophys. Biophys. Lett.* **1993**, *22*, 169–175.
17. Zettl, U.; Hoffmann, S. T.; Koberling, F.; Krausch, G.; Enderlein, J.; Harnau, L.; Ballauff, M. Self-Diffusion and Cooperative Diffusion in Semidilute Polymer Solutions As Measured by Fluorescence Correlation Spectroscopy. *Macromolecules* **2009**, *42*, 9537–9547.
18. Grabowski, C. A.; Mukhopadhyay, A. Diffusion of Polystyrene Chains and Fluorescent Dye Molecules in Semidilute and Concentrated Polymer Solutions. *Macromolecules* **2008**, *41*, 6191–6194.
19. Liu, R. G.; Gao, X.; Adams, J.; Oppermann, W. A Fluorescence Correlation Spectroscopy Study on the Self-Diffusion of Polystyrene Chains in Dilute and Semidilute Solution. *Macromolecules* **2005**, *38*, 8845–8849.
20. Cherdhirankorn, T.; Best, A.; Koynov, K.; Peneva, K.; Muellen, K.; Fytas, G. Diffusion in Polymer Solutions Studied by Fluorescence Correlation Spectroscopy. *J. Phys. Chem. B* **2009**, *113*, 3355–3359.
21. Wawrezinieck, L.; Rigneault, H.; Marguet, D.; Lenne, P. F. Fluorescence Correlation Spectroscopy Diffusion Laws to Probe the Submicron Cell Membrane Organization. *Biophys. J.* **2005**, *89*, 4029–4042.
22. Ruprecht, V.; Wieser, S.; Marguet, D.; Schuetz, G. J. Spot Variation Fluorescence Correlation Spectroscopy Allows for Superresolution Chronoscopy of Confinement Times in Membranes. *Biophys. J.* **2011**, *100*, 2839–2845.
23. Friedemann, K.; Turshatov, A.; Landfester, K.; Crespy, D. Characterization *via* Two-Color STED Microscopy of Nanostructured Materials Synthesized by Colloid Electrospinning. *Langmuir* **2011**, *27*, 7132–7139.
24. Ullal, C. K.; Schmidt, R.; Hell, S. W.; Egner, A. Block Copolymer Nanostructures Mapped by Far-Field Optics. *Nano Lett.* **2009**, *9*, 2497–2500.
25. Rust, M. J.; Bates, M.; Zhuang, X. Sub-Diffraction-Limit Imaging by Stochastic Optical Reconstruction Microscopy (STORM). *Nat. Methods* **2006**, *3*, 793–795.
26. Shroff, H.; Galbraith, C. G.; Galbraith, J. A.; Betzig, E. Live-Cell Photoactivated Localization Microscopy of Nanoscale Adhesion Dynamics. *Nat. Methods* **2008**, *5*, 417–423.
27. Willig, K. I.; Rizzoli, S. O.; Westphal, V.; Jahn, R.; Hell, S. W. STED Microscopy Reveals That Synaptotagmin Remains Clustered after Synaptic Vesicle Exocytosis. *Nature* **2006**, *440*, 935–939.
28. Haustein, E.; Schwille, P. Fluorescence Correlation Spectroscopy: Novel Variations of an Established Technique. *Annu. Rev. Biophys. Biomol. Struct.* **2007**, *36*, 151–169.
29. Dyba, M.; Hell, S. W. Focal Spots of Size Lambda/23 Open up Far-Field Florescence Microscopy at 33 nm Axial Resolution. *Phys. Rev. Lett.* **2002**, *88*, 163901.
30. Willig, K. I.; Kellner, R. R.; Medda, R.; Hein, B.; Jakobs, S.; Hell, S. W. Nanoscale Resolution in GFP-Based Microscopy. *Nat. Methods* **2006**, *3*, 721–723.
31. Moneron, G.; Hell, S. W. Two-Photon Excitation STED Microscopy. *Opt. Express* **2009**, *17*, 14567–14573.
32. Hein, B.; Willig, K. I.; Wurm, C. A.; Westphal, V.; Jakobs, S.; Hell, S. W. Stimulated Emission Depletion Nanoscopy of Living Cells Using SNAP-Tag Fusion Proteins. *Biophys. J.* **2010**, *98*, 158–163.
33. Berland, K. M.; So, P. T. C.; Gratton, E. 2-Photon Fluorescence Correlation Spectroscopy- Method and Application

to the Intracellular Environment. *Biophys. J.* **1995**, *68*, 694–701.

34. Fetters, L. J.; Hadjichristidis, N.; Lindner, J. S.; Mays, J. W. Molecular Weight Dependence of Hydrodynamic and Thermodynamic Properties for Well-Defined Linear Polymers in Solution. *J. Chem. Ref. Data* **1994**, *23*, 619–640.